IEEE Open Journal of the
Industrial Electronics Society

Received 12 November 2023; revised 15 December 2023; accepted 3 January 2024. Date of publication 5 January 2024;
date of current version 18 January 2024. The review of this article was arranged by Associate Editor A. Dianov.

Digital Object Identifier 10.1109/OJIES.2024.3350443

Robust Multiple-Fault Diagnosis of PMSM Drives Under Variant Operations and Noisy Conditions

MAHMOUD S. MAHMOUD [1] (Graduate Student Member, IEEE), VAN KHANG HUYNH [1], JAGATH SRI LAL SENANYAKA [2] (Member, IEEE), AND KJELL G. ROBBERSMYR [1] (Senior Member, IEEE)

[1]Faculty of Engineering and Science, University of Agder, 4879 Grimstad, Norway
[2]Norwegian University of Life Sciences, 1433 Ås, Norway

CORRESPONDING AUTHOR: MAHMOUD S. MAHMOUD (e-mail: mahmoud.sayed.m.eid@uia.no).

This work was supported in part by the Analytics for asset Integrity Management of Windfarms (AIMWind) under Grant 312486, through Research Council of Norway (RCN). AIMWind is a collaborative research project from the University of Agder, the Norwegian Research Center (NORCE), and TU Delft, with Origo Solutions as an advisory partner.

ABSTRACT With the rapid development of industrial applications using permanent magnet synchronous motors (PMSMs) and the Internet of Things, the demand for using robust fault diagnosis methods working in noisy conditions has increased significantly. The current data-driven methods depend mainly on deep learning (DL) models due to the effectiveness of automated feature extraction. However, these models have shallow depths compared with benchmark convolution neural networks, limiting their accuracy in final predictions, and they are established based on the hypothesis that the measured data are noiseless. Despite this, electric machinery is subjected to various noise sources that interfere with measurements during operation. This article proposes a new scheme combining a transfer-learned pretrained residual neural network (ResNet) and supervised machine learning (S-ML) to enhance the performance of DL models in noisy industrial environments. The effectiveness of the proposed scheme is validated using an in-house setup of a PMSM drive with demagnetization and intern-short circuit faults at variant operating conditions. The results show that the proposed method significantly reduced the computational burden by tenfold on average while improving the average accuracy to 96.84% across all the datasets compared with other DL and S-ML methods, with high robustness in noisy working conditions.

INDEX TERMS Deep transfer learning (TL), data-driven fault diagnosis, hybrid learning, permanent magnet synchronous motors (PMSMs), pretrained deep models, wavelet analysis.

NOMENCLATURE

AM	Attention-based multiscale module.
ANN	Artificial neural networks.
CNN	Convolution neural network.
CWT	Continuous wavelet transformation.
DBN	Deep belief network.
D-F	Demagnetization fault.
DL	Deep learning.
DRCN	Denoising residual convolutional network.
FDD	Fault detection and diagnosis.
FEM	Feature enhancement module.
HML	Hybrid machine learning.
ITSC	Intern-short circuit.
JAM	Joint attention module.
kNN	k-nearest neighbors.
MDM	multiscale denoising module.
NC	Normal healthy condition.
PMSMs	Permanent magnet synchronous motors.
ResNet	Residual neural network.
RUL	Remaining useful life.
SAE	Sparse autoencoder.
SC4-F	ITSC fault with 4% severity.
SC6-F	ITSC fault with 6% severity.
SGDM	Stochastic gradient descent with momentum.

S-ML Supervised machine learning.
SNR signal-to-noise ratio.
SVM Support vector machine.
TL Transfer learning.

I. INTRODUCTION

Recently, the rapid advancement of permanent magnet material and power electronics technology has led to the wide usage of PMSM in electric vehicles, aeroplanes, wind turbines, and in-house appliances [1]. PMSM drives have unique advantages of a high power-to-weight ratio, excellent dynamics, high torque, and a wide range of operating conditions. However, in the aforementioned applications, they are exposed to mechanical and thermal stresses under variant operations, leading to demagnetization and intern-short circuit faults (ITSC) [2]. In contrast to uniform demagnetization, which reduces all the magnets by the same ratio, local demagnetization occurs in a limited area of rotor poles, resulting in a magnetic asymmetry. These faults cause reduced motor efficiency. Therefore, diagnosing these faults early would reduce downtime, production losses and maintenance costs.

In recent years, many FDD methods have been significantly developed and are categorized into three main types: model-based, signal-based, and data-driven [3]. Model-based techniques require precise physical models and parameters of the implemented system to compute residuals between the model and the measurements, being difficult to obtain in reality [4]. Signal-based requires an identification of the fault-related characteristic frequencies or statistical features from the measured data [5], [6]. Thus, data-driven methods using machine learning have been developed rapidly due to their effectiveness in diagnosing multiple faults using historical data without prior knowledge of machine models or fault characteristics.

Much research has been carried out using data-driven methods for diagnosing faults in different applications using supervised machine learning (S-ML) and DL [7]. S-ML methods, such as SVM, kNN, and ANN, are frequently used in fault diagnosis due to significant advantages, such as easy implementation and low-computational burden [7]. However, the main challenge of using these models is choosing the features accurately to get high diagnostic accuracy. This process requires an expert and is usually time-consuming. Therefore, DL has been used to overcome this drawback. It can learn the features from the row data automatically [8]. Many DL methods, namely, CNN, DBN, and SAE, have been implemented in the field of fault diagnoses. For example, a convolutional variational autoencoder was used with frequency-weighted energy analysis and wavelet kernel convolutional block for fault identification of rolling bearings [9], a convolutional neural network was proposed with multiscale residual attention mechanism for bearing fault diagnosis from vibrational signals in noisy environments [10], and an attention-based multiscale denoising residual convolutional neural network method was introduced to assess the safety of mechanical equipment running under nonstationary conditions and noisy environments [11]. It incorporates a MDM to filter irrelevant information, a FEM to improve feature extraction, and a JAM to integrate discriminative features effectively. A robust diagnostic framework for bearings using a physics-informed solution was suggested in [12] using a unique physical modal-property-dominant-generated layer, which extracts modal properties from training and testing data, ensuring efficiency even with imperfect data. It introduces a domain-conversion layer to mitigate the impact of speed variations in bearing diagnostics. These studies significantly improved the diagnosis accuracy. However, it is still limited due to the requirement of a large amount of labeled data. Therefore, the structure of DL models has almost a few limited layers (5)–(7) [13]. Compared with the benchmark ImageNet-trained CNN models with many layers, fault-diagnosis DL models are very shallow and may not work effectively in noisy working environments. Furthermore, it is challenging to train multilayer deep CNN models without a large and well-organized training dataset. The bigger the number and size of hidden layers, the more parameters the model has, making it difficult to train large networks from scratch as it demands extensive labeled data and computational resources. Hyperparameter tuning, involving adjusting network architecture, learning rates, and dropout rates, is time-consuming and significantly affects diagnostic accuracy.

For these reasons, some studies used TL or hybrid machine learning (HML) to provide a suitable option to overcome the DL drawbacks. TL works by utilizing a deep network trained on labeled data for another application and then refining it for the current tasks. For instance, a deep TL approach was suggested using maximum mean discrepancy and SAE to improve the diagnosis accuracy in the bearing by recognizing similar features under varying operational conditions [14]. The study in [15] proposed a Bayesian semisupervised TL method for prognostic of RUL prediction across completely different machines using an active querying-based training data selection mechanism, whereas a TL method for RUL prediction of two different aerospace and bearing datasets using a consistency-based regularization was suggested in [16]. A digital twin-driven approach for intelligent assessment of gear surface degradation is suggested in [17], based on physical system measurements to monitor the dynamic response of the gear system as wear progresses. The method employs TL to apply knowledge from the digital twin models to assess surface wear in physical gearboxes nondestructively. This approach offers accurate wear severity assessment and expands the use of digital twin techniques in gear health management. Using TL only, however, requires that the target and source domains are similar, otherwise, the model may perform worse than if it had never been trained. To address this, recent research has focused on combining multiple machine learning techniques using HML to create more robust models without constraints for the source and target domains. The goal of HML is to improve the accuracy and performance of a model compared with using a single one. For instance, an HML method combining a convolutional autoencoder and deep CNN was proposed to improve the classification accuracy of

two mechanical fault simulations using a few shots [18], while a multilayer perceptron and CNN were combined to improve the diagnosis accuracy and robustness of gearbox mixed faults using feature-level data fusion [19]. Although both studies improved the classification accuracy, the first study requires an expert to select the domain knowledge features suitable for the diagnosis task, and the second may not be effective for diagnosing variant-operated PMSM drives since a large amount of data are required for training the deep models.

Despite the significant improvement in fault diagnosis by the current state-of-the-art methods presented in the literature, there are still major shortcomings as follows.

1) Most of these approaches are implemented in the hypothesis that the measured data are noiseless [9], [14], [15], [20]. However, electric machinery is subjected to a variety of noise sources that interfere with measurements during operation. Therefore, the existing techniques may be incapable of achieving adequate diagnosis results.
2) Prior research typically employs multiscale CNN architecture and denoising modules or physical-assisted models to investigate sufficient features and improve robustness [11], [12], [17]. These methods will, however, add an extensive number of parameters to the CNN model, which obviously requires a significant amount of time and computing power.
3) The other approaches depend on improving the robustness in noisy environments by fusing information from multiple sensors or classifier decisions [19], which increases the cost of the diagnosis scheme and the computational resources.

In addition, prior knowledge of features is required to assist DL models in extracting the features in a noisy environment [18].

In this framework, a new HML scheme is proposed using the residual neural network (ResNet) as a feature extractor while using S-ML models as classifiers. TL is used to accelerate the training of the deep ResNet architecture of the feature extractor and to acquire hierarchical features of the data. This is done using a deep ResNet-18 model trained previously on large datasets of natural images. The network architecture, model parameters, and hyperparameters are transferred from the pretrained network to be used in the fault diagnosis tasks as a features-extractor target model. The target network adopts the lower-level weights from the pretrained model and trains the higher level weights specifically for the fault diagnosis task. This provides the feature extractor with an optimal starting point and reduces the number of parameters to be updated, resulting in a substantial improvement in the training process. The multiple-fault diagnosis of faults under variable working conditions requires constructing source domain datasets large enough to represent the machine states under different working conditions. This will prevent overfitting and avoid errors during the mathematical operations of multilayer neural networks. Therefore, S-ML is combined with a tuned pretrained model as a feature extractor to overcome each model's shortcomings. The major contribution of this article is summarized as follows.

1) A new scheme combining a transfer-learned ResNet adopted as a feature extractor and S-ML as a classifier to tackle the problem of diagnosing multiple faults in noisy environments and variant conditions is introduced. To the best of the authors' knowledge, this low-computational cost scheme is applied for the first time to diagnose PMSM faults.
2) The proposed scheme is designed to use a benchmark ResNet-18 model as a feature extractor, which can automatically generate a discriminative feature for different faults with low computational burden and without prior knowledge of the features. In addition, the scheme has the flexibility to be adjusted to other domains according to data characteristics.
3) Four datasets, including different demagnetization and ITSC at variable operating conditions, are implemented to verify the effectiveness of the proposed scheme using one-phase current measurements.

Compared with other S-ML and DL models in this study, the proposed scheme has an outstanding performance for fault diagnosis tasks, as it reduced the computational burden during training and improved the classification accuracy under different noise conditions, making it an effective solution for fault diagnosis tasks. The rest of this article is organized as follows. Section II presents the proposed fault diagnosis scheme in detail. Section III introduces the experimental setup, faults implementation of demagnetization and ITSC, and different datasets. Section IV verifies the effectiveness of the proposed method. Finally, Section V concludes this article.

II. PROPOSED FAULT DIAGNOSIS SCHEME

The proposed fault diagnosis scheme uses deep TL ResNet and S-ML models to classify the faults at variable operating conditions with high accuracy, as shown in Fig. 1. The details of the scheme are explained as follows.

A. STAGE1: DATA PREPROCESSING

In the first stage, the one-phase current measurements were collected. The measured current data were subdivided into equal-size samples and converted to time–frequency images using CWT. The RGB time–frequency images were adjusted with a size of $224 \times 224 \times 3$ to fit the input layer of the pretrained model. This adjustment was done by duplicating the augmented one-channel Gray-scale images into three channels with a fixed base in each channel. The CWT is particularly efficient in analyzing the original signal at varying resolutions [21]. It is, therefore, commonly used for feature extraction in fault diagnosis applications. The wavelet transformation was executed by computing the inner product of the signal and a collection of wavelets that are generated by scaling and shifting the mother wavelet $\psi(t)$ as

$$\psi_{\delta,\varphi}(t) = \frac{1}{\sqrt{\delta}}\left(\frac{t-\varphi}{\delta}\right) \tag{1}$$

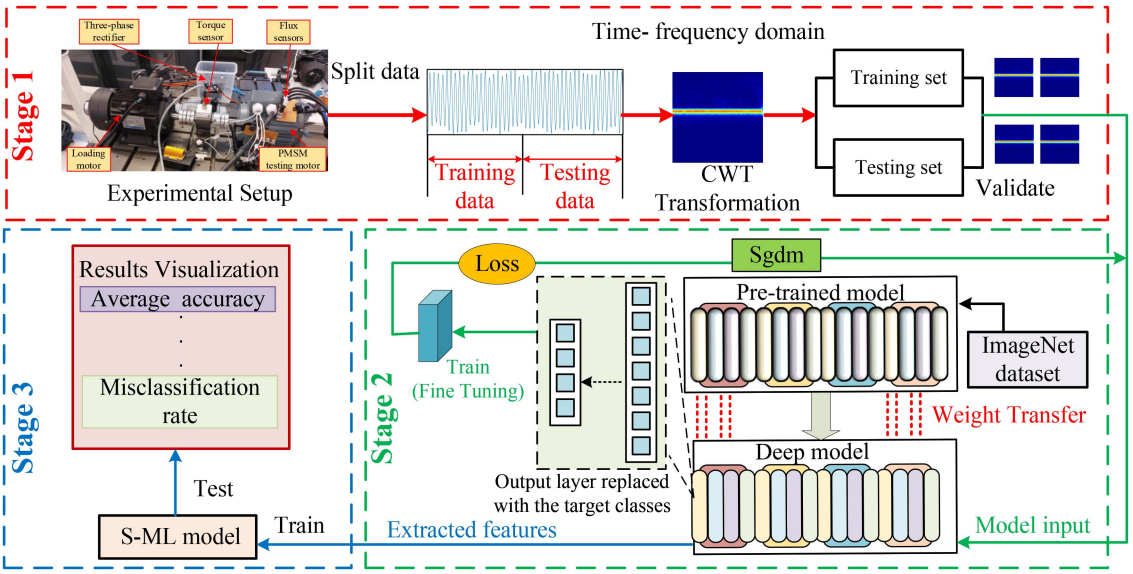

FIGURE 1. Proposed fault diagnosis scheme.

δ is the scaling factor that decreases as frequency increases, and φ is the parameter that defines the transition. The calculation of the CWT of a signal $x(t)$ involves performing a convolution between the signal and its complex conjugate and is defined as

$$C(\delta, \varphi) = \langle x(t), \psi_{s,\varphi} \rangle = \frac{1}{\sqrt{\delta}} \int x(t) \psi^* \left(\frac{t-\varphi}{\delta} \right) dt \quad (2)$$

where the complex conjugate of $\psi(\cdot)$ is represented by the notation $\psi^*(\cdot)$. The equation illustrates that the original signal can be divided into various frequency components. Using the wavelet parameters δ and φ, a collection of wavelet coefficients of the signal $x(t)$ was obtained and then mapped onto a 2-D plane to create time–frequency images [21].

B. STAGE2: FEATURE EXTRACTION USING DEEP TL

TL was then used for transferring weights from the pretrained model to our target feature-extractor deep model. This deep model was actively learned during the training process by calculating the loss and updating the model through the SGDM algorithm. A deep ResNet-18 pretrained model was tuned using the TL process. This pretrained model is a ResNet model that has a 72-layer architecture with 18 deep layers [22]. Since our time–frequency images differ from the pretrained model images, some convolution layers were modified to match our datasets and transfer the abstract features. The dimensions of the modified layers were adapted to fit the number of machine-healthy conditions, and their weights were randomly initialized. The learning layer weights were the only ones adjusted to reduce the error between the predicted and actual labels using the datasets as final refinements for the two convolution and fully connected layers. The pretrained model was trained afterward using 80% of the images from each dataset, with the remaining 20% split evenly for validation and testing purposes. The weights of the model were fine-tuned thereafter. The testing data were not used during the training or validation process. During the deep training of the feature extractor, the features are extracted from the CWT images using multiple convolution operations between the kernels and the input image and calculated as

$$a_{i,j} = a \left(\sum_{d=0}^{P-1} \sum_{m=0}^{S-1} \sum_{n=0}^{S-1} D_{m,n,d} x_{i+m,j+n,d} + \xi \right) \quad (3)$$

where x is the input image, which has a depth of P and position of (i, j) in the output feature map $a_{i,j}$. $x_{i+m,j+n,d}$ denotes the value at the location of (i, j) in the d depth. $D_{m,n,d}$ is the convolution kernel weight at the location of (m, n) in the dth depth. $S \times S$ is convolution kernel size, and b is the kernel bias. The pooling layer, which is responsible for the dimension reduction operation of the extracted features, can be described as

$$U_{i,j,k} = pool_{(m,n) \in G_{ij}} \left(x_{m,n,k} \right) \quad (4)$$

where $U_{i,j,k}$ is the value at (i, j) position in kth feature map after applying the pooling rule pool$(\cdot)$. $x_{m,n,k}$ is the node at (m, n) position of the target domain, and G_{ij} is the pooling of the target region at position (i, j). During the training of the pretrained model, the losses are minimized by cross entropy, which is described as

$$L_1(q, p) = -\sum_i \log(p_i) \quad (5)$$

where p is the output probability of the model and q is 0 or 1 depending on the label. This value is determined by the cross entropy that determines the error between true and predicated labels through updating a stochastic gradient descent with weight gradients by back-propagation. Once enough epochs had been completed, the deep architecture and all its parameters were saved for the optimized model. Afterward, the

deep features describing different machine conditions were extracted from the last pooling layer in the ResNet model.

C. STAGE3: SUPERVISED LEARNING BASED ON THE DEEP FEATURES

Finally, the deep-extracted features were used to train S-ML algorithms, and the categorical cross entropy for each class is calculated as

$$L_2 = -\sum y_{\text{true}} \times \log(y_{\text{pred}}) \tag{6}$$

where y_{pred} is the predicted probability distribution over classes and y_{true} is the true labels. The overall loss (L_o) of the proposed hybrid learning scheme is a combination of the feature extractor loss and S-ML loss and can be calculated as

$$L_o = \alpha L_1 + \beta L_2 \tag{7}$$

where α and β are weighting factors used to minimise the overall losses of the proposed hybrid scheme so that higher classification accuracy can be obtained. The suggested HML scheme improved the classification accuracy and computational burden during training (training time) since ResNet-18 was effectively used as a feature extractor to train the S-ML algorithms. Notably, the proposed approach learns fault signatures in an automated way and recognizes different machine working states from the original current signals.

III. EXPERIMENTAL VERIFICATION

A. EXPERIMENTAL SETUP

The experimental setup consists of a PMSM motor for testing connected to a loading motor via a torque transducer and flexible coupling as shown in Fig. 2(a). The testing motor is powered by an inverter while the output from the load is stabilized by a rectifier circuit to eliminate the ripples as shown in Fig. 2(b). A pulsewidth modulation (PWM) signal is used to regulate a brake chopper after amplifying the amplitude fourfold to be compatible with the data acquisition card. The brake chopper comprises a three-phase full-bridge rectifier, a 500 μF capacitor, an insulated-gate bipolar transistor, a variable resistor, and two flyback diodes. The brake chopper's variable resistor is set to 25 Ω and can consume up to 3.3 kW. The flyback diodes are connected across the resistor to provide a path for the stored energy. The required motor speed and torque during experiments are adjusted using a PWM signal defined by a duty cycle. The one-phase current measurements are carried out with a sampling frequency of 10 kHz. This configuration allows the analysis of different PMSM faults. Table 1 lists the rated parameters of the tested PMSM drive.

B. FAULTS IMPLEMENTATION

Implementing demagnetization faults is often carried out through partial removal of the magnets and substitution with nonmagnetic materials or by adding weaker magnets [23], [24]. Nevertheless, these solutions are unable to mimic the local demagnetization that arises from thermal cycling during the operation of PMSM drives, particularly in traction applications such as electric vehicles. Therefore, in this article, local

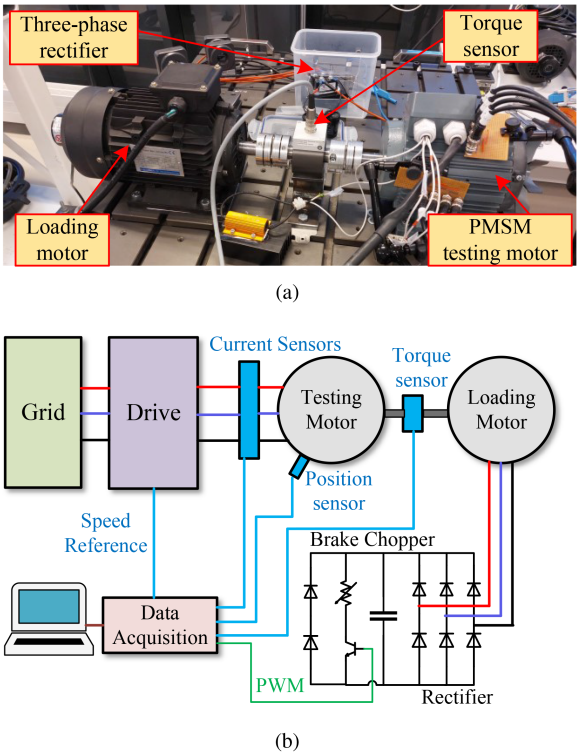

FIGURE 2. Experimental setup. (a) In-house test rig. (b) Schematic diagram.

TABLE 1. PMSM Rated Parameters

Parameter Description	Symbol	Value	Units
Rated power	P_N	2.2	[kW]
Rated torque	T_N	7	[Nm]
Rated speed	n_N	3000	[r/min]
Number of pole pairs	P_P	2	[-]
Frequency	f_{sN}	100	[Hz]
Stator current	I_{sN}	5	[A]
Nominal phase voltage	U_{sN}	280	[V]
Phase resistance	R_1	0.8	[Ω]
Phase horizontal inductance	L_{1H}	4.5	[mH]
Phase longitudinal inductance	L_{1S}	1.5	[mH]

demagnetization fault was implemented by heating specific regions in the rotor for a specific time using a stovetop while cooling the other regions with a cooling medium to protect the other poles from demagnetization [see Fig. 3(a)] [19], [25]. When specific regions of the rotor are heated to a certain temperature, the magnetic field strength of the poles is reduced, resulting in local demagnetization faults [26]. A magnetic field meter was used to monitor the flux reduction during the heat treatment process. The heat treatment time was selected based on the required demagnetization severity. Two regions on the north pole lost around 30.4% and 26.5% from their original field strength after the heat treatment, as shown in Fig. 3(c). During the diagnosis of the demagnetization fault, the thermally-treated rotor was positioned inside the stator of the testing motor. For implementing ITSC faults, the number of turns per phase was estimated to define the fault severity.

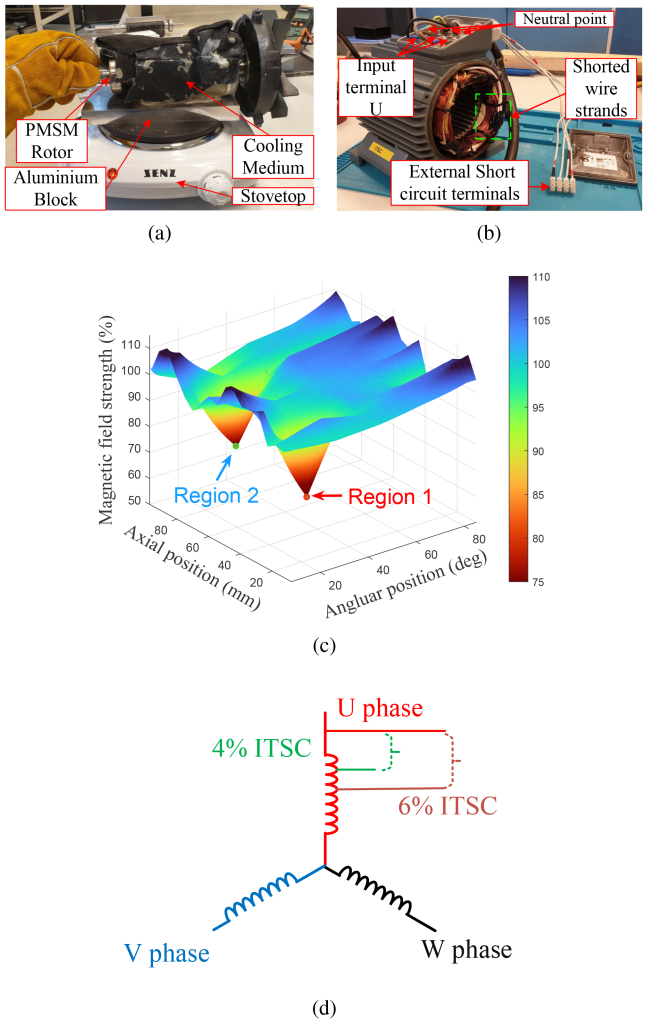

FIGURE 3. (a) Thermal treatment of rotor demagnetization. (b) ITSC windings fault. (c) Relative magnetic intensity of the demagnetized pole compared with the healthy pole. Regions 1 and 2 demagnetized by 30.4% and 26.5%, respectively. (d) Circuit diagram of ITSC faults implementation in phase U.

The neutral point was connected to the wire strands through the short-circuit terminals [see Fig. 3(b)]. The ITSC faults are implemented in motor phase U with the severity of 4% and 6% of the phase resistance, and the circuit diagram of the ITSC faults implementation is shown in Fig. 3(d).

C. DATASETS DESCRIPTION

One-phase stator current signals were collected at different operating conditions with sampling frequency $f_s = 10$ kHz. Every measurement file was recorded for 10 s and then split into 2 s so that each sample file had 20 000 data points, and three tests were performed repeatedly for each fault class. Four datasets were created to represent different PMSM operation conditions, as given in Table 2. The variable operations in each dataset are achieved by increasing the speed by 50 r/min every 2 s and recording data at different torque levels. The first dataset (DS-I) includes 60 operating points at

TABLE 2. Datasets Description

Name	No. of samples	No of operation conditions	Description
Ds-I	7200	60	Speeds: 1250∼2200 rpm Torque: 30 % , 60 % , 90 %
Ds-II	2400	20	Speeds: 1250∼2200 rpm Torque: 30 %
Ds-III	2400	20	Speeds: 1250∼2200 rpm Torque: 60 %
Ds-IV	2400	30	Speeds: 1600∼2200 rpm Torque: 90 % , 60%

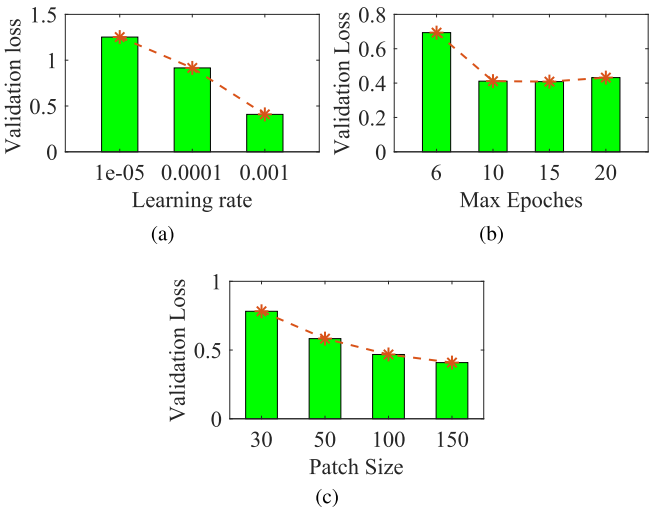

FIGURE 4. Hyperparameters tuning of the ResNet model. (a) Learning rate. (b) Max epochs. (c) Patch size.

20 speeds from 1250 to 2200 r/min and three different torques 30%, 60%, and 90% of the motor nominal torque. The dataset has 7200 samples, including 1800 samples for each fault type. Each dataset consists of four machine conditions: normal condition (NC), local demagnetization fault (D-F), ITSC faults with 4% severity (SC4-F), and 6% (SC6-F). The existence of variant-working conditions in each dataset is difficult to diagnose with high accuracy using only S-ML or DL methods because it requires many samples at each working condition enough to extract the features for different machine health conditions. Therefore, HML, consisting of deep transferred learning and S-ML, is presented in this article to overcome the challenges of classifying different faults with high accuracy, reducing the training time, and improving the robustness of the scheme to work in noisy conditions simultaneously.

IV. RESULTS AND DISCUSSIONS

A. EFFECT OF HYPERPARAMETERS ON DIAGNOSIS ACCURACY

To select the best parameters during the training of the pretrained models, multiple experiments were carried out by changing learning rates, max epochs and patch size while studying their effect on the validation losses as shown in Fig. 4. When the learning rate was 0.001, the pretrained DL model had the lowest validation losses. Four values were

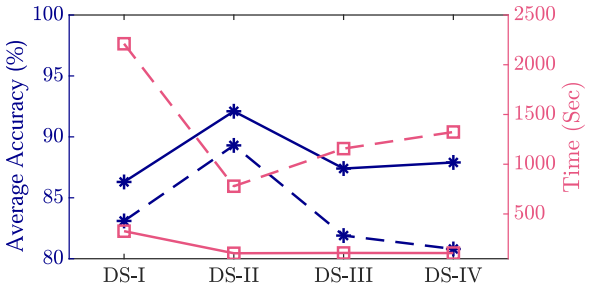

FIGURE 5. Average accuracy and elapsed time for training of deep-transferred ResNet model (Solid line) and scratch-trained D-CNN (Dash line).

studied for each max epoch and patch size to select the optimal parameters to reduce the losses during the training process. The validation loss was reduced significantly at 10 max epochs, before increasing again at 15 and 20 due to over-fitting. Therefore, the optimal parameters selected during the training of the deep transferred model were 0.001, 10, and 150 for learning rate, max epochs, and patch size, respectively.

B. SCRATCH-TRAINED AND PRETRAINED FEATURES EXTRACTOR COMPARISON

A comparison was carried out between using the ResNet-18 pretrained model with transferred weights and the same model trained from the beginning as a feature extractor for PMSM faults. The effect of the TF process on the training time and overall classification accuracy was studied as shown in Fig. 5. The duration of training was calculated from the beginning to the end of the process. In dataset DS-I, the pretrained model took six times less time to train than the scratch-trained model. In general, the training time of the pretrained model was less than the model trained from scratch across all the datasets by 10 times on average. It is obvious that dataset DS-I consumed more time during training because it has more operation conditions, requiring more time to extract the features during the DL process. In addition, the classification accuracy of the pretrained models was higher than the models trained from scratch, even though they had fewer parameters than pretrained models. The suggested pretrained model shows improved convergence rates and classification accuracy.

C. COMPARISON OF DIFFERENT PRETRAINED FEATURE EXTRACTORS

Several pretrained benchmark models used recently in the fault diagnosis tasks [8] were implemented, trained on dataset DS-II, and evaluated by validation losses and training time to study the effectiveness of the proposed ResNet-18 as a feature extractor for PMSM drive faults. The architecture and the specific characteristics of each model are described as follows.

1) AlexNet: Consists of eight layers, five of which are convolutional layers followed by max-pooling layers, and the last three are fully connected layers [27].

TABLE 3. Hardware and Software Setups

Components	Description
Operating System	Windows 10, 64-bit
CPU	Intel(R) Xeon(R) CPU E5-2630 v4 @ 2.20GHz
GPU	NVIDIA GeForce RTX 3070 Ti
RAM	32.0 GB
CUDA Version	11.7.64
MATLAB Version	MATLAB R2022b

TABLE 4. Comparison of Different Feature Extractors Benchmark Models

	Number of deep layers	Losses	Training time (s)
AlexNet	8	0.9	438
ResNet-50	50	0.6	609
VGG-16	16	0.4	650
ResNet-18	18	0.3	105
SqueezeNet	18	0.7	452

2) VGG-16: It has 16 layers, including 13 convolutional layers and three fully connected layers [28]. The architecture consists of 3×3 convolutional filters with small stride and max-pooling layers, which help to capture fine-grained details in images. However, it has been largely surpassed by deeper and more efficient architectures in recent years, such as the various models in the ResNet.
3) ResNet-50: Consists of 50 layers and includes a series of convolutional layers [29], followed by multiple residual blocks, each containing several convolutional layers and skip connections. By using residual connections, very deep neural networks can be trained without encountering the vanishing gradient issue.
4) ResNet-18: Is a specific type of ResNet with 18 layers [22]. Compared with ResNet-50, it serves as a relatively compact and efficient architecture while still benefiting from the advantages of deep residual networks.

These models were implemented and trained in MATLAB R2022b and executed on the Windows 10 operating system. The hardware and software configurations used are listed in Table 3. Five benchmark models are compared in Table 4, and the results show that the validation losses and the training time of ResNet-18 were the lowest among the other models due to the effectiveness of the residual blocks to improve the learning of the network to extract the features during training (see Fig. 6). ResNet-18 has a shallower architecture compared to ResNet-50, which reduces computational cost without losing much accuracy. In addition, it has demonstrated strong generalization capabilities, which is important for applications where the model needs to perform well on a variety of inputs beyond the training dataset. Although SqueezeNet and AlexNet have a similar or smaller number of deep layers, the losses and training time were higher than the ResNet-18 network. Therefore, ResNet-18 was used as an efficient feature extractor for different PMSM faults to train S-ML models. It

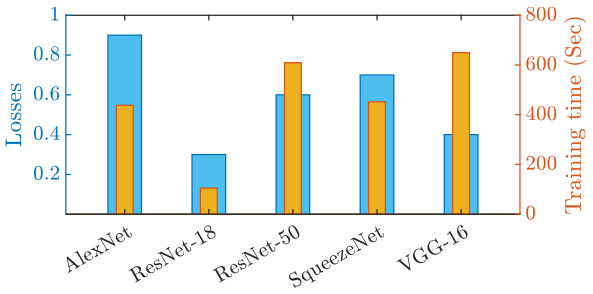

FIGURE 6. Performance of different feature extractors. The losses and training time are highlighted in blue and yellow, respectively.

should be noted that the percentage of training time in ResNet-18 compared with the time used to collect the measurement samples of the DS-II dataset is 2.18%. This is considered a significant advantage in the proposed method and can be utilized in industrial applications that have an extensive amount of historical data that need to be trained frequently.

D. RESULTS AND ANALYSIS OF THE PROPOSED HYBRID MODELS

In this study, hybrid learning was carried out by extracting the deep-learned features from the pretrained ResNet model and training S-ML algorithms on these features, extracted from the last max-pooling layer. This combination of deep and supervised models reduces the overall losses significantly so that a better diagnosis accuracy can be obtained. The effectiveness of the hybrid models will be discussed through a comparative study of the overall classification accuracy of eight different machine learning models as follows.

1) D-PR: Deep pretrained model using ResNet-18 and was tuned using TL.
2) D-SC: Deep CNN model had the same number of deep layers as ResNet and was trained from the beginning.
3) SF-SVM, SF-KNN, SF-CNN: Supervised SVM, kNN, convolutional neural network models trained using 14 statistical features in time and frequency domain, namely, mean, standard division, rms, clearance factor, shape factor, kurtosis, skewness, impulse factor, crest factor, frequency mean, frequency standard division, frequency variance, frequency RMS, frequency skewness, and calculated as in [18].
4) H-SVM, H-KNN, H-CNN: The proposed hybrid SVM, kNN, convolutional neural network models trained using the deep TL features extractor and S-ML models as classifiers.

Ac_o represents the accuracy for all categories and is calculated as

$$Ac_o = \frac{\sum_{i=1}^{M} x_{\text{test,correct}}^{(i)}}{N} \tag{8}$$

where $x_{\text{test,correct}}$ represents the number of samples in the ith category test sample that were classified correctly and N stands for the total number of samples in the test set.

TABLE 5. Fault Diagnosis Results of Different Datasets

Model	DS-I	DS-II	DS-III	DS-IV	AVG
D-PR	87.64	90.87	91.21	86.67	89.1
D-SC	84.03	88.38	86.19	83.75	85.59
H-CNN	98.61	97.93	94.14	92.5	**95.8**
H-SVM	95.14	95.85	93.72	92.92	**96.87**
H-KNN	100	98.34	96.65	92.5	**94.41**
SF-CNN	61.53	79.36	77.93	80	74.71
SF-KNN	89.72	82.57	78.03	82.08	83.1
SF-SVM	67.57	80.91	76.67	79.58	76.18

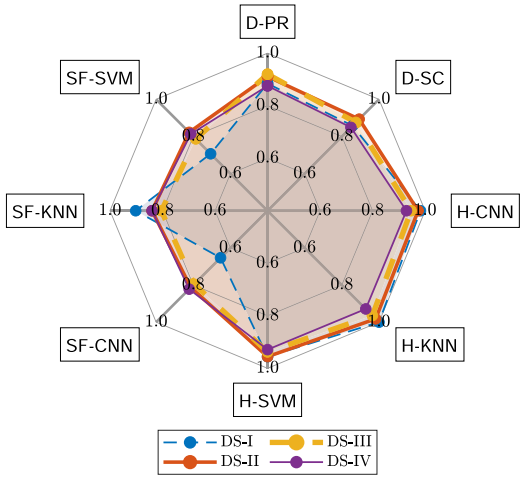

FIGURE 7. Average overall accuracy of different methods at the four datasets.

As given in Table 5 and Fig. 7, the proposed hybrid models have the highest accuracy in all the datasets. Although the S-ML models were trained on statistical features from the time–frequency domain, these models do not have a high accuracy compared with the other models because the statistical features are ineffective in classifying the faults at the datasets with variable-working conditions. It is observed that the SF-CNN and SF-SVM models of the DS-I dataset have the lowest diagnostic accuracy among all the others due to having the largest number of operating conditions. To increase the diagnosis accuracy of the supervised models, the amount of training data samples needs to be quite large at each working condition. Therefore, the pretrained ResNet-18 DL model was used as a DL feature extractor because it has low losses during the validation and a short training time compared with the D-CNN model trained from the beginning. The residual blocks in the ResNet-18 improve the mining of the deep features during the training process. Therefore, the proposed models could effectively extract the wavelet-based time–frequency features from the images during training.

To better demonstrate the feature extraction performance of the pretrained ResNet-18 model, the output feature vectors were reduced to 2-D by t-SNE. Fig. 8 shows the t-SNE representation of the learned features of the datasets at the first max-pooling layer and the last layer (Softmax) in the

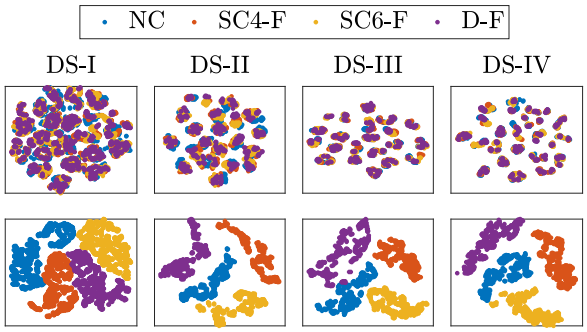

FIGURE 8. 2-D visualization of the extracted features from the first max-pooling layer and the last layer (Softmax) of the proposed scheme.

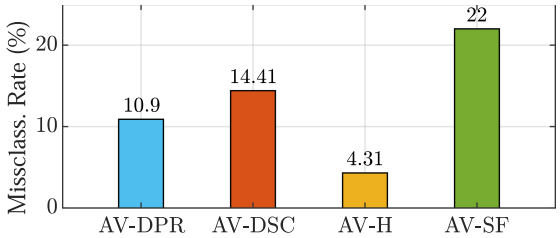

FIGURE 9. Average misclassification rate of the four approaches across different datasets.

pretrained model architecture. It can be seen that in the first max-pooling layers, the time–frequency features extracted from the images are overlapped due to the multiple operating conditions in each dataset. The deep ResNet-18 model characterized different faults effectively after the last layer. However, the model is prone to problems, such as overfitting under small samples of each operating condition, and the deep-learned features are subjected to errors during the calculation of the multilayer neural network. Therefore, extracting these learned features in the hybrid learning process to train S-ML models as classifiers is more effective in classifying the machine faults working at variable operations with high accuracy.

The proposed hybrid learning models are highly accurate compared with supervised, DL and pretrained models trained on the same sample number. Through the four datasets, the proposed fault diagnosis method using hybrid learning (AV-H) reduced the average misclassification rate compared with deep pretrained (AV-DPR), scratch-trained (AV-DSC) by 6.59%, 10.1%, while supervised models (AV-SF) have the highest rate, 17.69% higher than AV-H (see Fig. 9). To further demonstrate the effects of the proposed hybrid methods at different machine states, the testing data of the dataset DS-I were visualized by confusion matrices as shown in Fig. 10. The number of test samples for each health condition was 180. The horizontal axes are the predicated labels, and the vertical axes are the true labels. The results show that the proposed hybrid learning gives the best diagnostic performance for the different classes of PMSM drives working in variant operations.

TABLE 6. Testing Average Accuracy Under Different Noisy Conditions

Model	0 dB	20 dB	25 dB	30 dB
H-SVM	93.9% ±0.65	94.2% ±0.9	95.3% ±0.87	96.3% ±0.5
H-KNN	94.3% ±0.32	94.8% ±0.76	96.7% ±0.65	97.56% ±0.98
H-CNN	94.08%±0.57	95.38%±0.76	96.1%±0.51	96.7%±0.93
D-PR	84.12%±1.2	85.07%±0.9	87.04%±1.3	88.11%±1.79

E. TESTING ROBUSTNESS OF THE PROPOSED SCHEME IN DIFFERENT NOISY CONDITIONS

The robustness of the proposed hybrid learning scheme was tested to extract the weak features from the noisy background by adding different noise levels to the motor current measurements. The level of the added noise is expressed by the signal-to-noise ratio (SNR) as

$$\mathrm{SNR} = 10\log\left(\frac{P_{\mathrm{signal}}}{P_{\mathrm{noise}}}\right)(\mathrm{dB}) \tag{9}$$

where P_{signal} is the original signal power and P_{noise} represents the noise signal power. The scheme was trained using four types of noisy signals. For each SNR ratio, three datasets were used for training, validation, and testing. Three experiments were carried out, and the mean and standard division of the accuracy were calculated.

Table 6 gives the accuracy of the proposed method at three hybrid learning models compared with the pretrained ResNet-18 model. The proposed scheme consistently maintains accuracy levels above 93.9% with a standard deviation of 0.65% in various noisy environments. The accuracy of the proposed method rises when the SNR increases. The reason is that at higher SNR levels, the signal becomes clearer and easier to recognize in contrast to noise, allowing the proposed scheme to extract the relevant features from the feature extractor effectively. Therefore, it is important to test the robustness of the model to work in different noisy environments. Compared with other D-PR, the proposed method enhanced the robustness of the diagnostic accuracy in noisy environments by extracting the features effectively through the deep features extractor while training the S-ML models on these features to classify the faults as shown in Fig. 11.

In the framework of PMSM drives working at variant operating conditions, the proposed fault diagnosis method has the following advantages: first, the proposed HML approach effectively extracts rich and discriminative features from time–frequency images, leading to higher accuracy in identifying faults compared to traditional methods, such as DCNN and S-ML. Second, the computational burden during the training of the hybrid models is reduced significantly to extract the features in a short time by 10× since the training is based on transferring the weights from the pretrained model on another domain to the time–frequency fault diagnosis domain. The proposed scheme is applicable with automated feature extraction for different fault diagnosis tasks without prior knowledge of the domain and can be adjusted according to data characteristics. Finally, the scheme is robust to work in different noisy environments with high classification accuracy.

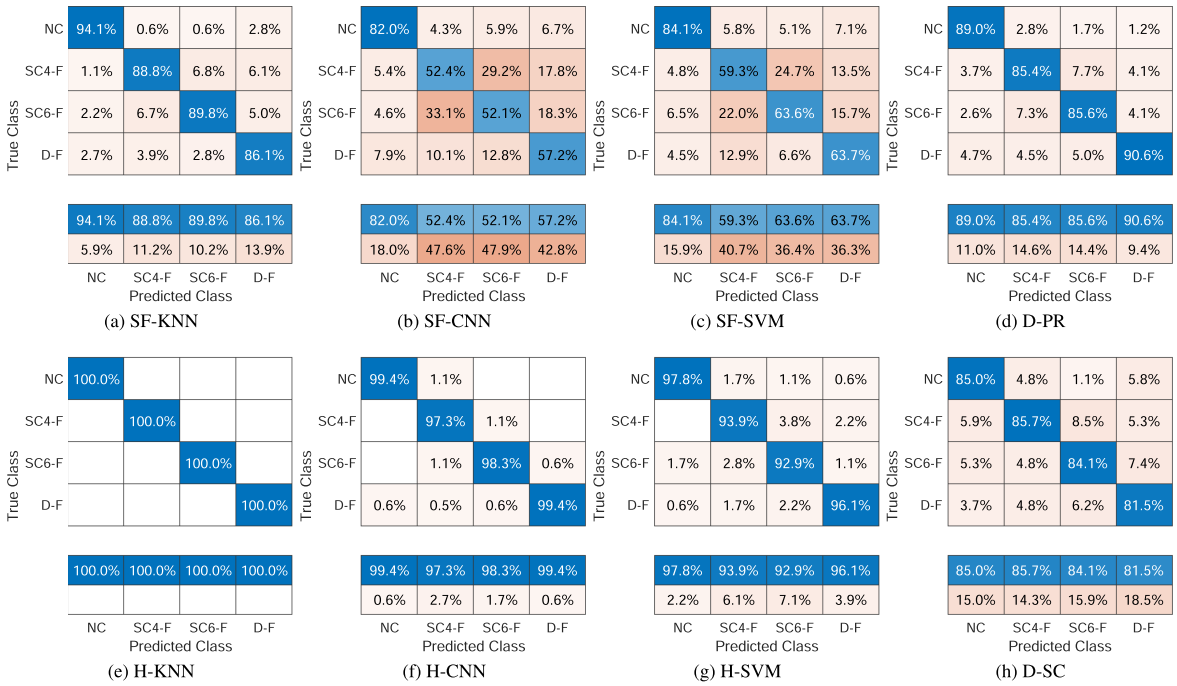

FIGURE 10. **Confusion charts of different faults for DS-I.**

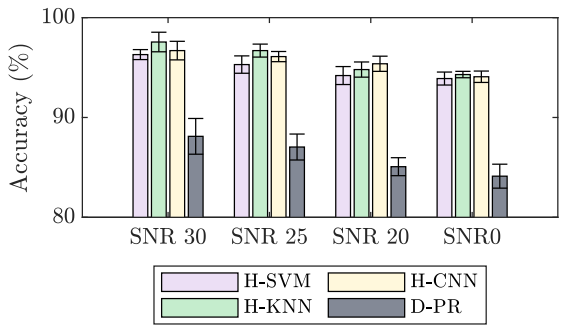

FIGURE 11. **Accuracy of the proposed method under different levels of noise.**

V. CONCLUSION

This article proposed a robust fault diagnosis scheme for PMSM drives using a combination of a pretrained deep-TL model as a feature extractor and S-ML models as classifiers to tackle the problem of diagnosing multiple faults during working at variant operations. The suggested hybrid-learning scheme enhanced the interoperability of the conventional machine-learning methods to extract the features of different machine faulty status while reducing the elapsed time in training by ten times on average. The multiple-fault classification accuracy is significantly improved since supervised learning was used to reduce the error of the multilayer feature extractor model. In addition, the scheme is remarkably more robust during operating in noisy environments. The proposed method reached an average accuracy of 96.84% across all datasets regardless of noise in the collected data while consistently maintaining accuracy levels above 93.9% with a standard deviation of 0.65% in various noisy environments.

Although the proposed scheme has achieved significant results compared with the other methods in the scope of this study, some limitations still need further development, such as dealing with the unknown classes of faults, that may occur in PMSM and classifying the faults under low-labeled data. In future research, a further study will address these limitations while maintaining the proposed scheme's robustness and low computational cost.

REFERENCES

[1] S. Singh, S. Singh, and A. Tiwari, "PMSM drives and its application: An overview," *Recent Adv. Elect. Electron. Eng. (Formerly Recent Patents Elect. Electron. Eng.)*, vol. 16, no. 1, pp. 4–16, 2023.

[2] R. Li, H. Fang, D. Li, R. Qu, S. Yang, and R. Wang, "A search coil design method of PMSM for detection of inter-turn short-circuit fault," *IEEE Trans. Ind. Electron.*, vol. 71, no. 4, pp. 3964–3974, 2023, doi: 10.1109/TIE.2023.3274879.

[3] S. Lu, J. Lu, K. An, X. Wang, and Q. He, "Edge computing on IoT for machine signal processing and fault diagnosis: A review," *IEEE Internet Things J.*, vol. 10, no. 13, pp. 11093–11116, Jul. 2023.

[4] Y. Han, S. Chen, C. Gong, X. Zhao, F. Zhang, and Y. Li, "Accurate SM disturbance observer-based demagnetization fault diagnosis with parameter mismatch impacts eliminated for IPM motors," *IEEE Trans. Power Electron.*, vol. 38, no. 5, pp. 5706–5710, May 2023, doi: 10.1109/TPEL.2023.3245052.

[5] M. Alam and S. Payami, "A novel control-independent online fault diagnosis of interturn short circuits in SRMS using signal injection technique," *IEEE Trans. Ind. Electron.*, vol. 70, no. 3, pp. 2157–2167, Mar. 2023, doi: 10.1109/TIE.2022.3169709.

[6] M. Orviz et al., "Demagnetization detection and severity assessment in PMSMs using search coils exploiting machine's symmetry," *IEEE Trans. Ind. Appl.*, vol. 59, no. 4, pp. 4021–4034, Jul./Aug. 2023, doi: 10.1109/TIA.2023.3267772.

[7] W. Zhang, D. Yang, and H. Wang, "Data-driven methods for predictive maintenance of industrial equipment: A survey," *IEEE Syst. J.*, vol. 13, no. 3, pp. 2213–2227, Sep. 2019, doi: 10.1109/JSYST.2019.2905565.

[8] Y. Lei, B. Yang, X. Jiang, F. Jia, N. Li, and A. K. Nandi, "Applications of machine learning to machine fault diagnosis: A review and roadmap," *Mech. Syst. Signal Process.*, vol. 138, 2020, Art. no. 106587.

[9] X. Yan, D. She, and Y. Xu, "Deep order-wavelet convolutional variational autoencoder for fault identification of rolling bearing under fluctuating speed conditions," *Expert Syst. Appl.*, vol. 216, 2023, Art. no. 119479. [Online]. Available: https://www.sciencedirect.com/science/article/pii/S0957417422024988
[10] L. Jia, T. W. S. Chow, Y. Wang, and Y. Yuan, "Multiscale residual attention convolutional neural network for bearing fault diagnosis," *IEEE Trans. Instrum. Meas.*, vol. 71, 2022, Art. no. 3519413, doi: 10.1109/TIM.2022.3196742.
[11] Y. Xu, X. Yan, K. Feng, X. Sheng, B. Sun, and Z. Liu, "Attention-based multiscale denoising residual convolutional neural networks for fault diagnosis of rotating machinery," *Rel. Eng. System Saf.*, vol. 226, 2022, Art. no. 108714.
[12] Q. Ni, J. Ji, B. Halkon, K. Feng, and A. K. Nandi, "Physics-informed residual network (PIResNet) for rolling element bearing fault diagnostics," *Mech. Syst. Signal Process.*, vol. 200, 2023, Art. no. 110544.
[13] R. Zhao, R. Yan, Z. Chen, K. Mao, P. Wang, and R. X. Gao, "Deep learning and its applications to machine health monitoring," *Mech. Syst. Signal Process.*, vol. 115, pp. 213–237, 2019.
[14] L. Wen, L. Gao, and X. Li, "A new deep transfer learning based on sparse auto-encoder for fault diagnosis," *IEEE Trans. Syst., Man, Cybern. Syst.*, vol. 49, no. 1, pp. 136–144, Jan. 2019, doi 10.1109/TSMC.2017.2754287.
[15] R. Zhu, W. Peng, D. Wang, and C.-G. Huang, "Bayesian transfer learning with active querying for intelligent cross-machine fault prognosis under limited data," *Mech. Syst. Signal Process.*, vol. 183, 2023, Art. no. 109628. [Online]. Available: https://www.sciencedirect.com/science/article/pii/S0888327022007166
[16] S. Siahpour, X. Li, and J. Lee, "A novel transfer learning approach in remaining useful life prediction for incomplete dataset," *IEEE Trans. Instrum. Meas.*, vol. 71, 2022, Art. no. 3509411, doi: 10.1109/TIM.2022.3162283.
[17] K. Feng, J. Ji, Y. Zhang, Q. Ni, Z. Liu, and M. Beer, "Digital twin-driven intelligent assessment of gear surface degradation," *Mech. Syst. Signal Process.*, vol. 186, 2023, Art. no. 109896.
[18] T. Zhang, J. Chen, S. He, and Z. Zhou, "Prior knowledge-augmented self-supervised feature learning for few-shot intelligent fault diagnosis of machines," *IEEE Trans. Ind. Electron.*, vol. 69, no. 10, pp. 10573–10584, Oct. 2022, doi: 101109/TIE.2022.3140403.
[19] J. S. L. Senanayaka, H. Van Khang, and K. G. Robbersmyr, "Multiple classifiers and data fusion for robust diagnosis of gearbox mixed faults," *IEEE Trans. Ind. Informat.*, vol. 15, no. 8, pp. 4569–4579, Aug. 2019, doi: 10.1109/TII.2018.2883357.
[20] S. Xiang, J. Zhou, J. Luo, F. Liu, and Y. Qin, "Cocktail LSTM and its application into machine remaining useful life prediction," *IEEE/ASME Trans. Mechatron.*, vol. 28, no. 5, pp. 2425–2436, Oct. 2023, doi: 10.1109/TMECH.2023.3244282.
[21] P. Gangsar and R. Tiwari, "Signal based condition monitoring techniques for fault detection and diagnosis of induction motors: A state-of-the-art review," *Mech. Syst. Signal Process.*, vol. 144, 2020, Art. no. 106908, doi 10.1016/j.ymssp.2020.106908.
[22] K. He, X. Zhang, S. Ren, and J. Sun, "Deep residual learning for image recognition," in *Proc. IEEE Conf. Comput. Vis. Pattern Recognit.*, 2016, pp. 770–778, doi: 10.1109/CVPR.2016.90.
[23] J.-C. Urresty, J.-R. Riba, M. Delgado, and L. Romeral, "Detection of demagnetization faults in surface-mounted permanent magnet synchronous motors by means of the zero-sequence voltage component," *IEEE Trans. Energy Convers.*, vol. 27, no. 1, pp. 42–51, Mar. 2012.
[24] F. Huang et al., "Demagnetization fault diagnosis of permanent magnet synchronous motors using magnetic leakage signals," *IEEE Trans. Ind. Informat.*, vol. 19, no. 4, pp. 6105–6116, Apr. 2023, doi: 10.1109/TII.2022.3165283.
[25] S. Attestog, J. S. L. Senanayaka, H. V. Khang, and K. G. Robbersmyr, "Robust active learning multiple fault diagnosis of PMSM drives with sensorless control under dynamic operations and imbalanced datasets," *IEEE Trans. Ind. Informat.*, vol. 19, no. 9, pp. 9291–9301, Sep. 2023, doi: 10.1109/TII.2022.3227628.
[26] S. S. Moosavi, A. Djerdir, Y. A. Amirat, and D. A. Khaburi, "Demagnetization fault diagnosis in permanent magnet synchronous motors: A review of the state-of-the-art," *J. Magnetism Magn. Mater.*, vol. 391, pp. 203–212, 2015.
[27] S. Sun et al., "Fault diagnosis of conventional circuit breaker contact system based on time–frequency analysis and improved AlexNet," *IEEE Trans. Instrum. Meas.*, vol. 70, 2021, Art. no. 3508512, doi: 10.1109/TIM.2020.3045798.
[28] S. Shao, S. McAleer, R. Yan, and P. Baldi, "Highly accurate machine fault diagnosis using deep transfer learning," *IEEE Trans. Ind. Informat.*, vol. 15, no. 4, pp. 2446–2455, Apr. 2019, doi: 10.1109/TII.2018.2864759.
[29] L. Wen, X. Li, and L. Gao, "A transfer convolutional neural network for fault diagnosis based on resnet-50," *Neural Comput. Appl.*, vol. 32, pp. 6111–6124, 2020.

MAHMOUD S. MAHMOUD (Graduate Student Member, IEEE) received the B.Sc. degree in mechatronics engineering, Helwan University, Cairo, Egypt, in 2013, the M.Sc. degree in advanced mechanical engineering and robotics, Ritsumeikan University, Kyoto, Japan, in 2019. He is working toward the Ph.D. degree in mechatronics engineering with the Department of Engineering Sciences, University of Agder, Grimstad, Norway.

His current research interests include intelligent fault diagnosis, electric machines, signal processing, deep learning models, and digital twins.

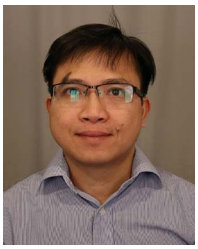

VAN KHANG HUYNH received the B.Sc. degree in electrical engineering from the Ho Chi Minh City University of Technology, Ho Chi Minh City, Vietnam, in 2002, the M.Sc. degree in electrical engineering from Pusan National University, Busan, South Korea, in 2008, and the D.Sc. (Tech.) degree in electrical engineering from Aalto University, Espoo, Finland, in 2012.

From 2013 to 2019, he was an Associate Professor in electrical power engineering with the University of Agder, Grimstad, Norway, where he is currently a Professor with the Department of Engineering Sciences. His research interests include electrical machines, condition-based maintenance, and applied power electronics.

JAGATH SRI LAL SENANYAKA (Member, IEEE) received the B.Sc. degree in electrical and information engineering from the University of Ruhuna, Galle, Sri Lanka, in 2007, the M.B.A. degree in technology management from the University of Moratuwa, Moratuwa, Sri Lanka, in 2012, and the M.Sc. degree in renewable energy and the Ph.D. degree in mechatronics from the University of Agder, Grimstad, Norway, in 2014 and 2020, respectively.

From 2021 to 2022, he was a Postdoctoral Research Fellow with the University of Agder. Currently, he is an Associate Professor with the Faculty of Science and Technology, Norwegian University of Life Sciences, Oslo, Norway. His current research interests include fault diagnosis and control of electric powertrains, power electronics, and renewable energy.

KJELL G. ROBBERSMYR (Senior Member, IEEE) received the M.Sc. and Ph.D. degrees in mechanical engineering from the Norwegian University of Science and Technology, Trondheim, Norway, in 1985 and 1992, respectively.

He is currently a Professor of machine design. Earlier, he was the head of Dynamics Research Group, and he is currently a Director of Top Research Centre Mechatronics with the University of Agder, Grimstad, Norway. His main research interests include machine design, rotating machines, condition monitoring, and vehicle crash simulations.